Electromagnetic modeling of the copper layers influence for AC losses in ReBCO coated conductors based on T-A formulation

Electromagnetic modeling of the copper layers influence for AC losses in ReBCO coated conductors based on T-A formulation

Inês S. P. Peixoto, *Student Member*, *IEEE*, Sofia Viarengo, *Student Member*, *IEEE*, João F. P. Fernandes, *Member, IEEE*, Fabio Freschi, *Senior Member*, *IEEE*, Laura Savoldi, *Member, IEEE*, and Silvio Vaschetto, *Senior Member, IEEE*

***Abstract*—ReBCO coated conductors are a promising solution to be integrated in superconducting electrical machines due to their high transport current under high magnetic fields. However superconducting armature windings will be subjected to AC fields and AC currents, resulting in non-negligible loss. These losses need to be estimated to achieve feasible designs since they strongly decrease the performance of the superconductors, affecting machine operation. In numerical models, ReBCO tapes are often represented by a superconducting thin sheet due to their high aspect ratio. Nonetheless, research shows that at high currents and/or frequencies, the influence of the stabilizing copper layers in the coated conductor's losses can become significant. In this paper, we propose a 2D electromagnetic model based on the *T-A* formulation to include the effect of copper layers on current distribution and on the evaluation of losses through Finite Elements Method models. A ReBCO tape is investigated when different currents and magnetic fields (perpendicular to the tape surface) are imposed, and the magnetization and transport losses of the superconductors show good agreement with homogenized *T - A* formulation, experimental and analytical results.**

***Index Terms*— AC loss, finite element method, Coated superconductors, ReBCO, *T-A* formulation.**

I. Introduction

High temperature superconductors (HTS) have shown the potential to extend energy conversion devices' efficiency and power density. The second generation (2G) coated conductors manifest high current carrying capacity and improved in-field performance, making them a promising choice for designing devices with increased magnetic loading and reduced weight [1], [2]. However, in electrical motors, generators, and transformers, superconductors (SCs) are exposed to AC currents or alternating magnetic fields and, thus, manifest non-negligible losses. Given the necessity of a cooling system capable of dissipating the SC losses and keeping the materials at cryogenic temperatures to ensure safe operation, practical superconducting electrical devices can only be realized after precise loss estimation in SC components. To estimate the 2G tape electromagnetic performance through finite element methods (FEM), the *T-A* formulation is recognized by its accuracy and reduced computational cost [3]. The reduced complexity of this formulation is achieved by assuming that all current flows in the SC layer and modelling the coated conductor as a SC layer of negligible thickness [4], [5]. This allows for modelling the superconducting domain with the current vector potential, **T**, perpendicular to the tape's surface. This approximation can become inaccurate at high frequencies or high currents because of non-negligible losses on the copper layers of the coated conductor [6]-[8]. The non-superconducting materials of the SC tape can be modeled in *T-A* based models for loss estimation through the homogenization method proposed in [9]. Yet, this method does not allow for differentiation of the loss contribution from the different HTS tape layers.

This paper proposes a multilayer modeling method to include the current sharing and additional loss contribution from the copper stabilizing layers of the coated conductor. By integrating the circuit laws through boundary conditions, the multilayered model allows analyzing different layers of the SC tape separately and better identify optimal operating conditions for coated conductor tapes in electrical devices. The multilayered *T-A* formulation is presented, and numerical results are compared with those of the single-layer and homogenized *T-A* models, as well as experimental and analytical results.

II. Numerical Models

In this research, the coated conductors considered are fabricated by SuperPower [10]. The tapes several layers with their geometrical parameters are depicted in Fig. 1. This study focuses exclusively on the influence of HTS and copper layers on the tape losses. Other layers, including silver, buffer, and substrate, are not included in the simulations due to their expected low contribution to the tape losses [6]. The copper stabilizing layers are assigned a resistivity of $\rho_{Cu} = 2.33 \cdot$

This work has been partly carried out within the framework of the EUROfusion Consortium, funded by the European Union via the Euratom Research and Training Programme (Grant Agreement No 101052200 — EUROfusion). Views and opinions expressed are however those of the author(s) only and do not necessarily reflect those of the European Union or the European Commission. Neither the European Union nor the European Commission can be held responsible for them. (Corresponding author: Inês S. P. Peixoto)

Inês S. P. Peixoto, Sofia Viarengo, Fabio Freschi, Laura Savoldi and Silvio Vaschetto, are with the Politecnico di Torino, Dipartimento Energia "G. Ferraris", Torino, 10129, Italy (e-mail: ines.peixoto@polito.it, sofia.viarengo@polito.it, fabio.freschi@polito.it, laura.savoldi@polito.it, silvio.vaschetto@polito.it).

João F. Fernandes is with Departamento de Engenharia Electrotécnica e de Computadores, University of Lisbon, Instituto Superior Técnico, Lisbon Portugal (e-mail: joao.f.p.fernandes@tecnico.ulisboa.pt)

Color versions of one or more of the figures in this article are available online at http://ieeexplore.ieee.org

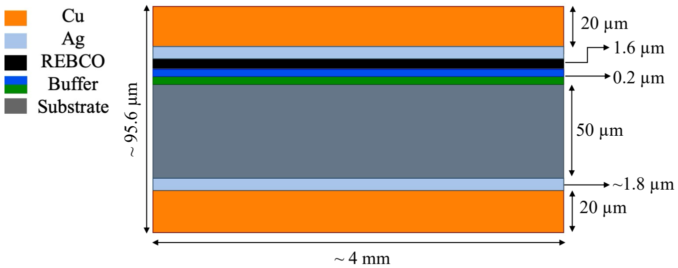

Fig. 1. Illustration of the coated conductor cross section depicting its several layers (not to scale).

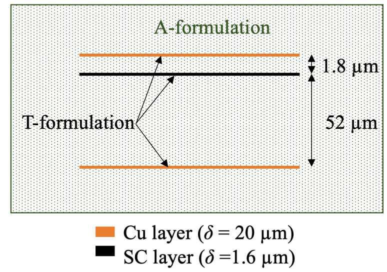

Fig. 2. Illustration of the 2D tape model geometry, including the superconducting and the copper layers.

$10^{-9}\,\Omega m$ at 77 K [7]. The electrical behavior of the superconductor is described using the widely accepted power law in (1) [11].

$$\mathbf{E} = E_0 \left(\frac{|\mathbf{J}|}{J_c(\mathbf{B})}\right)^{(n-1)} \frac{\mathbf{J}}{J_c(\mathbf{B})} \tag{1}$$

In (1) E_0 is the critical electric field, defined by convention as $100\ \mu V/m$, n is the SC exponential constant imposed as 21. The critical current density J_c is magnetic field $\mathbf{B}$ dependent according to Kim's model in (2) [12].

$$J_c(\mathbf{B}) = J_{c0}\,\frac{1}{1+|\mathbf{B}|/B_0} \tag{2}$$

In (2) J_{c0} is the critical current density in self-field, corresponding to a critical current I_{c0} of 162 A, and B_0 is the magnetic field that lowers the critical current density J_c by half equal to 140 mT. The tape parameters, I_{c0}, B_0 and n were measured and the tape model was characterized at 77 K by the procedure described in [7].

A. The multi-layer T-A formulation

Accounting for the high aspect ratio of tapes, the thin-sheet approximation has been shown to significantly reduce the degrees of freedom of the electromagnetic problem while maintaining high accuracy for loss calculation [3]. This means that the current is assumed to flow in the conducting layers tangentially to the tape surface [13], [14]. The thin sheet approximation is applied in the HTS and copper layers (with air in between) and its geometry is depicted in Fig. 2.

The numerical model for the multi-layer *T-A* formulation is based on the definition of the potential vector $\mathbf{T}$ in the tape domain, $\Omega_{tape} = \Omega_{SC} + \Omega_{Cu}$. In all other domains Ω_A, the magnetic vector potential $\mathbf{A}$ is defined as in (3). The Faraday's law in (4) is solved [15].

$$\nabla \times \mathbf{T} = \mathbf{J} \text{ in } \Omega_{tape}, \quad \nabla \times \mathbf{A} = \mathbf{B} \text{ in } \Omega_A \tag{3}$$

$$\nabla \times \mathbf{E} = -\,{}^{\partial \mathbf{B}}/_{\partial t} \tag{4}$$

Current is applied in the tapes by homogeneous Dirichlet boundary conditions on one side of the tape edges, whereas a global constraint, defined in (5), defines the current sharing between layers.

$$\mathrm{I} = \int J_z \delta_{SC} dw_{sc} + \int J_z \delta_{Cu} dw_{Cu} \tag{5}$$

In (5), w_{SC} and w_{Cu} denotes the superconducting and copper layers width, while δ denotes the thickness of each layer. To ensure the layers are in electric parallel and guarantee current sharing a boundary condition is imposed to define the equipotentiality. Applying the Stokes' theorem to the definition of the current vector potential in (3), then (6) is obtained [3].

$$\iint_S \mathbf{J} \cdot \mathbf{n}\, d\Omega_{tape} = \oint_L \mathbf{T} \cdot dl\ = I \tag{6}$$

In (6) L denotes the path formed by the boundary edges of the conductor and $\mathbf{n}$ the normal unit vector. The total electric field in each layer of the tape will be the sum of an induced component and an applied component. However, when $\mathbf{E}$ is integrated in the tape's width, the induced component of the electric field is canceled, see (7) and (8). Similarly, when the current density is described by (9), the induced components along the tape's width is canceled, giving the relation in (10).

$$\int \left(\mathbf{E}_{ap_{SC}} + \mathbf{E}_{ind_{SC}}\right) dw_{SC} = \int \mathbf{E}_{ap_{SC}} dw_{SC} \tag{7}$$

$$\int \left(\mathbf{E}_{ap_{Cu}} + \mathbf{E}_{ind_{Cu}}\right) dw_{Cu} = \int \mathbf{E}_{ap_{Cu}} dw_{Cu} \tag{8}$$

$$\mathbf{E}_{Cu} = \rho_{Cu}\mathbf{J}_{Cu} = \rho_{Cu} \int \left(\mathbf{J}_{ap_{Cu}} + \mathbf{J}_{ind_{Cu}}\right) dw_{Cu} \tag{9}$$

$$\int \mathbf{E}_{Cu} dw_{Cu} = \int \mathbf{E}_{ap_{Cu}} dw_{Cu} = \rho_{Cu} \int \mathbf{J}_{ap_{Cu}} dw_{Cu} \tag{10}$$

Therefore, the same applied electric field can be imposed in the SC and copper layers as shown in (11). Using the definition in (6) and (11), the Dirichlet boundary condition at the copper layer edge according to *T-A* formulation, ensuring the same electric field is present in all the tape layers, is defined in (12).

$$\int \mathbf{E}_{ap_{SC}} dw_{SC} = \int \mathbf{E}_{ap_{Cu}} dw_{Cu} = \rho_{Cu} \int \mathbf{J}_{ap_{Cu}} dw_{Cu} = \frac{\rho_{Cu} I_{ap_{Cu}}}{h_{Cu}} \tag{11}$$

$$T_{Cu} = \frac{I_{ap_{Cu}}}{\delta_{Cu}} = \frac{1}{\rho_{Cu}} \int \mathbf{E}_{ap_{SC}}\, d\Omega_{SC} \tag{12}$$

B. Homogenized model

The model is implemented in the commercial software COMSOL Multiphysics and compared and verified against a T-A homogenized model developed in [16]. In the latter the tape is treated as a single material considering the contribution of the YBCO and copper layers. The equivalent electric conductivity σ_{eq} is computed as an electric parallel among the copper and HTS layers weighted on the cross section A.

$$\sigma_{eq} = \frac{\sum_{j=1}^{N} \sigma_j A_j}{\sum_{j=1}^{N} A_j} \tag{13}$$

The subscript j is referred to the j-th layer, and N is the number of layers within the tape. The YBCO electric conductivity is computed from the power law in (1).

IV. Experimental Setup

To determine the HTS parameters in (1)-(2), namely J_{c0}, n and B_0. experimental measurements are conducted on a tape, both in DC and AC to calibrate the model. During the tests, the tape was submerged in a liquid nitrogen (LN_2) bath within an EPS foam container, as shown in Fig. 3.

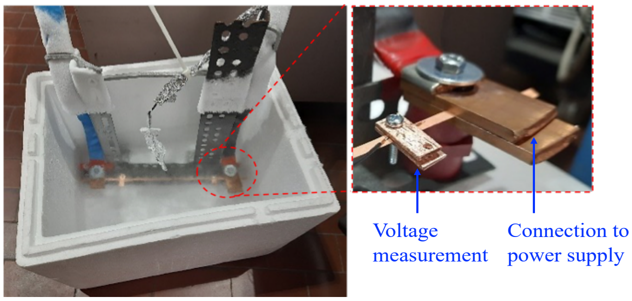

Fig. 3. ReBCO tape in the LN2 bath and detail of the copper plates used for the voltage drop measurement and for connecting at the power supply connection.

A. DC measurements

The nonlinear *E-J* curve of the superconducting tape was measured by supplying the coated conductor with a DC current. A DC power source was used to supply currents ranging from 0 to 170 A. Voltage measurements across the superconducting tape were conducted using an HP 34401A multimeter with high precision up to 10^{-6} V. The critical current value, I_{c0}, was determined at the point where an electric field of $100\ \mu\mathrm{V/m}$ was measured.

B. AC measurements

To measure the HTS tape losses (superconducting hysteresis and eddy currents losses and copper losses), which occur when a superconducting tape is supplied with AC currents under self-field conditions (commonly referred to as transport losses [17]), the circuit shown in Fig. 4 was utilized [7]. The HTS tape was connected to the secondary side of a transformer with a turn ratio equal to 100:1, to adapt the voltage and current values generated by the sinusoidal power supply for the tape test.

When an AC current is applied to the superconducting (SC) tape, the resulting voltage, $v_{SC}(t)$, measured across the tape consists of two components: a resistive component and a nonlinear inductive component. The resistive component arises primarily from hysteresis losses and eddy currents within the SC tape and Joule losses in the copper layers, whereas the inductive component is predominantly associated with the magnetic flux linked by the closed loop formed by the voltmeter connections and the SC strip. The voltage on the SC tape can be expressed as shown in equations (14) and (15). In (15), the inductive component of the measured voltage in (14) is defined. The '*internal*' magnetic flux $\Psi(t)$ represents the leakage flux that affects the SC, it contributes to the non-linear self and mutual inductances between the conducting layers inside the tape. The '*external*' $\Psi_{ext}(t)$ refers to the magnetic flux linked between the tape and the voltmeter connection.

$$v_{SC}(t) = Ri(t) + \frac{\mathrm{d}\Psi(t)}{\mathrm{d}t} \qquad (14)$$

$$\Psi(t) = \Psi_{int}(t) + \Psi_{ext}(t) = \Psi_{int}(t) + L_{ext} \cdot i(t) \qquad (15)$$

To compute the transport losses on the SC tape, only the resistive component in (14) must be considered. Therefore, a compensation coil with adjustable mutual coupling M was used to measure only the resistive voltage component in (14) [18]. Hence, the magnetic flux $\Psi(t)$ can be written as in (16), where M is the mutual inductance of the compensation coil.

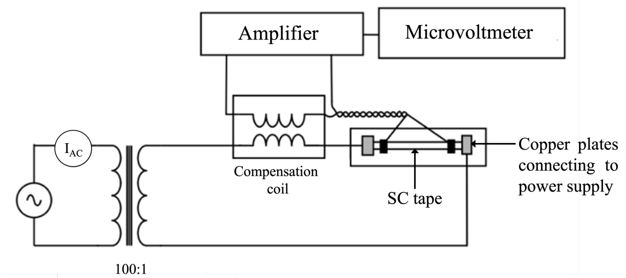

Fig. 4. Circuit schematic for AC transport loss measurements on the superconducting tape.

$$\Psi(t) = \Psi_{int}(t) + (L_{ext} - M) \cdot i(t) \qquad (16)$$

The AC losses per unit length are obtained by the integral average value of the instantaneous power as in (17), where l *is* the distance from the voltage pick-up tips [19].

$$\mathrm{P}_{measured} = \frac{1}{l \cdot T} \int_0^T v_{SC}(t) \cdot i(t)\, dt \qquad (17)$$

The measured AC losses are compared to those obtained by the FEM model of the SC tape. The parameter set that allows to achieve good convergence between the FEM and measured AC loss curve has been used for the calibrated FEM model as in [7]. The relevant values are listed in Section II. By the conducted measurements it has also been verified that the critical current well matches the data provided by the manufacturer for the considered 30 m length tape (equal to 162 A, with a minimum guaranteed value of 158 A).

V. Results

The applicability of the multi-layer model was evaluated by comparing numerical results with the experiments described in the previous section and analytical solutions in the literature. The superconducting tapes were analyzed for AC transport current losses and magnetization losses.

A. Transport Current Losses

When a superconductor is supplied with an alternate current, it exhibits transport current losses. Norris initially derived the analytical solution for transport loss P_{TN} for an applied current $I_T < I_c$ [20]. An extension of this model was recently proposed that considers both the hysteretic and resistive characteristics of the superconducting tape in the overcritical regime $I_T > I_c$, P_{TF} [7]. The analytical results for P_{TN} and P_{TF} for thin strip tapes are stated in (18) for $I_T < I_c$ and in (19) for $I_T > I_c$.

$$P_{TN} = \frac{\mu_0 f I_{c0}^2}{\pi}\left[(1-i)\ln(1-i) + (1+i)\ln(1+i) - i^2\right] \qquad (18)$$

In (18), i is the ratio between the amplitude of the transport current and the critical current at self-field, I_T/I_c, and f is the supply current frequency.

$$P_{TF} = \frac{\mu_0 f I_{c0}^2}{\pi}\left[(1-F)\ln(1-F) + (1+F)\ln(1+F) - F^2\right] + {i^{n+1} I_c E_0 (n+1)!}\Big/{2^{n+1}\left(\frac{n+1}{2}\right)!}\ , \quad F = \min(i,1) \qquad (19)$$

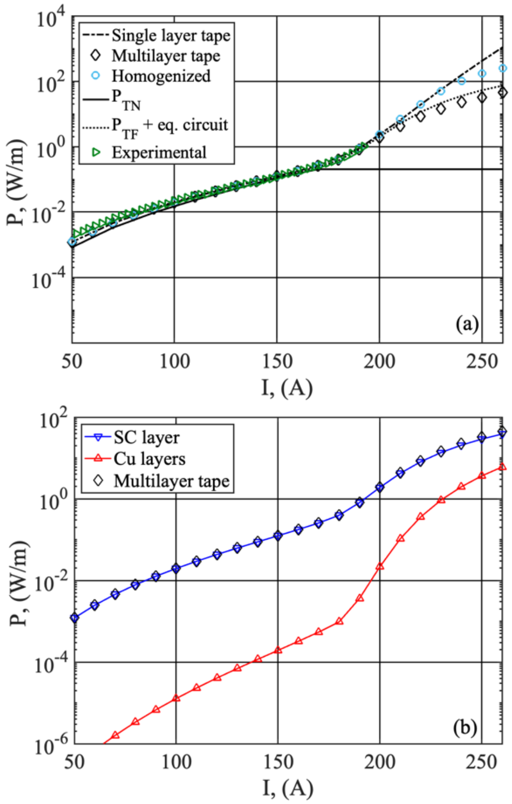

Fig. 5. (a) Comparison between analytical, FEM and experimental AC losses per unit length at 77 K, 50Hz for the measured REBCO tape. (b) Loss contribution from each layer determined by the multilayer model.

The loss component in (19) can be used to estimate the superconductor resistivity in an overcritical current regime. Using the result in (19), the superconductor contribution to the losses can be analyzed with the copper layers in an equivalent electrical circuit [7]. In the 2D FEM models, the tape losses per unit length are computed using (20), where w and δ are the tape's width and thickness respectively.

$$p(t) = \int_w \boldsymbol{E} \cdot (\boldsymbol{J}\delta)\, dw, \quad P_{ac} = \frac{1}{T}\int_0^T p(t)dt \qquad (20)$$

In Fig. 5a, the experimental, analytical (P_{TN} and P_{TF}+eq. circuit) and FEM AC loss results are plotted for the HTS tape. Fig. 5b shows the multilayer model different contributions from the SC and copper layers. Note that experimental results are limited to 175 A supply to keep the tape from quenching. All FEM models show good agreement with experimental data bellow the overcritical current regime. For currents above 175 A, however, the multilayer model has the closest agreement with analytical results obtained by the equivalent circuit model in [7] which separates the current flowing between the copper and HTS while maintaining the same voltage across layers. The single-layer tape has a loss that becomes considerably larger at high currents than the multilayered and homogenized models. This is due to the losses computed in FEM, which incorrectly considers only an HTS and thus correspond to the superconducting loss in (19). This result further supports the assumption that at high currents, the copper resistivity must be considered.

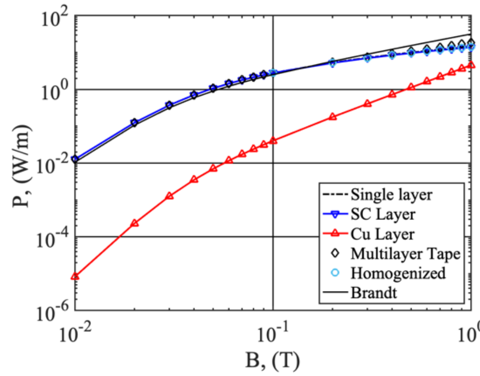

Fig. 6. Magnetization AC losses per unit length at 50Hz.

The homogenized model increased contribution to the tape losses is introduced due to computation of the tape current with an averaged current penetration depth, from the contribution of the SC and copper layers, as opposed to the multilayered model which has different current penetration for each of the layers, that are modelled separately. This discrepancy between the homogenized and the multilayered models indicate that accuracy of analyses in HTS tapes is increased when the tape's multilayered structure is considered.

B. Magnetization Losses

The results for a single tape subject to a sinusoidal magnetic field perpendicular to the tape surface are plotted in Fig. 6. There is good agreement between numerical models and the analytical solution provided by Brandt's solution for magnetization losses in a superconducting strip subject to an alternate magnetic field applied perpendicular to the tape wide surface (4 mm) P_M (W/m) in (21) [21].

$$P_M = \mu_0 w^2 f J_c \delta H_0 g\left(\frac{H_0}{H_c}\right) \qquad (21)$$

In (21) H_0 is the applied magnetic field amplitude, H_c is the characteristic field, $I_{c0}/w\pi$, and $g(x)$ is given by (22).

$$g(x) = (2/x)\ln\cosh(x) - \tanh(x) \qquad (22)$$

In the magnetization case, the difference between the single-layer and the multilayered models is less noticeable; however, the copper layer loss trend indicates that as the magnetic field increases, the contribution of the stabilizing layers to the total loss can become equivalent to that of the SC layer.

VI. Conclusion

An electromagnetic model based on *T-A* formulation for coated conductor ReBCO tapes has been developed. The model considers the superconducting and copper layers for the evaluation of AC losses. The current sharing and parallel connection between the tapes different layers is guaranteed through the imposition of the boundary conditions on the copper and superconducting layers. The model has been verified and compared against other established formulation, analytical and experimental results, showing a very good agreement with references. In perspective, the model can be used for more complex geometry and exploit to explore multiple design for HTS applications.

REFERENCES

[1] I. S. P. Peixoto, S. Vaschetto, J. F. P. Fernandes, P. J. Da Costa Branco, A. Tenconi and A. Cavagnino,” Modeling Approach for Superconducting AC Windings: Case Study on Axial Flux PM Machines,” 2023 IEEE Energy Conversion Congress and Exposition (ECCE), Nashville, TN, USA, 2023, pp. 3790-3795.

[2] M. Biasion, J. F. P. Fernandes, S. Vaschetto, A. Cavagnino and A. Tenconi, “Superconductivity and its Application in the Field of Electrical Machines,” 2021 IEEE International Electric Machines & Drives Conference (IEMDC), Hartford, CT, USA, 2021, pp. 1-7.

[3] D. J. Gameiro Carvalho, F. Ferreira da Silva, J. F. P. Fernandes and P. J. da Costa Branco, “Finite-element recipes for HTS-coated conductors and HTS tape topologies,” *Supercond. Sci. Technol.*, vol. 36, no. 10, 2023.

[4] K.Takeuchi, N. Amemiya, T. Nakamura, O. Maruyama and T. Ohkuma, “Model for electromagnetic field analysis of superconducting power transmission cable comprising spiraled coated conductors,” *Supercond. Sci. Technol.*, vol. 24, no. 8, pp. 085014, 2011.

[5] H. Zhang, M. Zhang and W. Yuan, “An efficient 3D finite element method model based on the T–A formulation for superconducting coated conductors,” *Supercond. Sci. Technol.*, vol. 30, no. 2, pp. 024005, 2016.

[6] H. Zhang et al., “Modelling of electromagnetic loss in HTS coated conductors over a wide frequency band,” *Supercond. Sci. Technol.*, vol. 33, pp. 025004, 2020.

[7] J. F. P. Fernandes, L. F. D. Bucho, F. Ferreira da Silva, I. S. P. Peixoto, S. Vaschetto and P. J. Costa Branco, “Alternative analytical models for HTS tapes considering their AC hysteretic and resistive losses,” *Supercond. Sci. Technol.* vol. 37 pp. 035004

[8] F. Ferreira da Silva, J. F. P. Fernandes, and P. J. da Costa Branco, " Superconducting Electric Power Systems: R&D Advancements," in *Energies*, vol. 15, no. 19, pp. 7350, 2022.

[9] Zermeno, Victor M. R., et al. “Calculation of Alternating Current Losses in Stacks and Coils Made of Second Generation High Temperature Superconducting Tapes for Large Scale Applications.” *J. Appl. Phys.*, vol. 114, no. 17, 2013, pp. 173901.

[10] SuperPower Inc., [Online]. Available: http://www.superpower-inc.com

[11] D. A. Cardwell, D. C. Larbalestier, A. Braginski, Handbook of Superconductivity: Characterization and Applications, 2nd ed., vol.3 CRC Press, 2022

[12] D. X. Chen; R. B. Goldfarb, “Kim model for magnetization of type-II superconductors,” *J. Appl. Phys*., vol. 66, pp. 2489–2500, 1989.

[13] H. Tsuboi, and K. Kunisue, “Eddy Current Analysis of Thin Plates Taking Account of the Source Current Distributions and Its Experimental Verifications,” *IEEE Trans. Magn.* vol.27 pp. 4020–4023, 1991.

[14] M. Nii, N. Amemiya, and T. Nakamura, “Three-Dimensional Model for Numerical Electromagnetic Field Analyses of Coated Superconductors and Its Application to Roebel Cables,” *Supercond. Sci. Technol.* vol.25 pp. 95011, 2012.

[15] F. Huber et al., “The T-A formulation: an efficient approach to model the macroscopic electromagnetic behaviour of HTS coated conductor applications,” *Supercond. Sci. Technol.*, vol. 35, pp. 043003, 2022.

[16] S. Viarengo et al., "A New Coupled Electrodynamic T – A and Thermal Model for the Critical Current Characterization of High-Temperature Superconducting Tapes and Cables," *IEEE Access*, vol. 11, pp. 107548-107561, 2023.

[17] F. Grilli, E. Pardo, A. Stenvall, D. N. Nguyen, W. Yuan and F. Gömöry, "Computation of Losses in HTS Under the Action of Varying Magnetic Fields and Currents," *IEEE Trans. Appl. Supercond.*vol. 24, no. 1, pp. 78-110, Feb. 2014, Art no. 8200433

[18] J. Zhu, Z. Zhang, H. Zhang, M. Zhang, M. Qiu and W. Yuan, "Electric Measurement of the Critical Current, AC Loss, and Current Distribution of a Prototype HTS Cable," *IEEE Trans. Applied Supercond.*, vol. 24, no. 3, pp. 1-4, June 2014.

[19] J. -H. Kim, C. H. Kim, G. Iyyani, J. Kvitkovic and S. Pamidi, "Transport AC Loss Measurements in Superconducting Coils," *IEEE Trans. Appl. Supercond.*, vol. 21, no. 3, pp. 3269-3272, June 2011.

[20] J W. T. Norris. “Calculation of hysteresis losses in hard superconductors carrying ac: isolated conductors and edges of thin sheets”. *J. Phys. D: Appl. Phys.*, vol. 3, no. 4, 1970.

[21] E. H. Brandt, and M. Indenbom, “Type-II-superconductor strip with current in a perpendicular magnetic field,” *Phys. Rev. B*, vol. 48, pp. 12893–12906, Nov. 1993.